

Finite Element Analysis of CFRP- Reinforced Concrete Beams

Análisis de elementos finitos de Vigas de Hormigón Armado CFRP

A. Sakbana *, M. Mashreib ^{1**}

* Misan University – Amarah, IRAQ

** Thi-Qar University – Nasiriya, IRAQ

Fecha de Recepción: 20/01/2020

Fecha de Aceptación: 23/05/2020

PAG 148-169

Abstract

This study concerns with flexural behavior of RC beams strengthened by carbon fiber reinforced polymer (CFRP) using finite element method (FEM). ABAQUS program has been used in this research. The load-deflection relationship, crack pattern, strain in the concrete at mid-span section of the beam and failure modes of all tested beams are studied. After validation of FEM model, parametric studies are presented to assess the effect of the compressive strength of concrete, thickness, and length of CFRP, and the presence of CFRP on stress in steel bars. From the current results, it can be obtained that the flexural capacity of RC beams strengthened with CFRP increased by 6.6% for beam strengthened by EBR and to 108.8% for beam strengthened by near surface mounted (NSM) compared to the reference beams. According to parametric studies, it is found that by increasing the compressive strength of concrete from 30 MPa to 70 MPa, the beam capacity increase by 25.6%, while increasing the length of CFRP from 600 mm to 900 mm leads to increase the beam capacity by 12.7%. Increasing thickness of CFRP sheet from 0.11 mm to 0.5 mm leads to an increase in the stiffness and the flexural capacity of the beam by 47.9%. Also, the results of this study approved that the strengthening of RC beams by CFRP laminates using the NSM technique is more efficient than externally bonded reinforcement (EBR) techniques and this is agreed with the experimental results. Finally, it can be concluded that the finite element model provides good accuracy compared to the experimental results and ACI-440 results.

Keywords: FEM (Finite Element Method); CFRP (Carbon Fiber Reinforced Polymer); Behavior; Flexure; Beam

Resumen

Este estudio se refiere al comportamiento de flexión de vigas RC fortalecidas con polímero reforzado con fibra de carbono (CFRP) utilizando el método de elementos finitos (MEF). El programa ABAQUS se ha utilizado en esta investigación. Se estudia la relación carga-deflexión, patrón de grietas, deformación en el concreto en la sección del tramo medio de la viga y los modos de falla de todas las vigas probadas. Después de la validación del modelo MEF, se presentan estudios paramétricos para evaluar el efecto de la resistencia a la compresión del concreto, el grosor y la longitud de CFRP, y la presencia de CFRP en la tensión de las barras de acero. A partir de los resultados actuales, se puede obtener información que la capacidad de flexión de las vigas RC reforzadas con CFRP aumentó en un 6.6% para vigas reforzadas por EBR y a 108.8% para vigas reforzadas por montaje cerca de la superficie (NSM) en comparación con las vigas de referencia. Según estudios paramétricos, se encuentra que, al aumentar la resistencia a la compresión del concreto de 30 MPa a 70 MPa, la capacidad de la viga aumenta en un 25.6%, mientras que el aumento de la longitud de CFRP de 600 mm a 900 mm conduce a aumentar la capacidad de la viga en 12,7%. El aumento del grosor de la lámina de CFRP de 0,11 mm a 0,5 mm conduce a un aumento de la rigidez y la capacidad de flexión de la viga en un 47,9%. Además, los resultados de este estudio probaron que el fortalecimiento de las vigas RC por laminados CFRP utilizando la técnica NSM es más eficiente que las técnicas de refuerzo unido externamente (RUE) y esto está de acuerdo con los resultados experimentales, se puede concluir que el modelo de elementos finitos proporciona una gran precisión en comparación con los resultados experimentales y los resultados de ACI-440.

Palabras clave: MEF (Metodo de Elementos Finitos); CFRP (Polimero Reforzado con Fibra de Carbono); Comportamiento; Flexión; Viga

1. Introduction

Reinforced concrete structures usually have to face modification and improvement of their performance throughout their service life. The most contributing factors are modification in their use, new design standards, deterioration because of corrosion in the steel caused by exposure to an aggressive environment and accident events like earthquakes .

The improvement of the performance of RC members throughout their service life can do it by strengthening or retrofitting and repairing of the member. Replacement of the structure might need determinate disadvantages like high prices of materials and labors, a stronger environmental impact and inconvenience because of interruption of the function of the structure. Therefore, it is preferring to repair or rehabilitation of the member. Using CFRP to strengthen RC beams is a common type of strengthening in the field of structural engineering (Obaidat, 2011); (Bodzak, 2019).

The use of CFRP in strengthening RC beams has become an important alternative method and more effective than other methods such as strengthening by steel plate. CFRP has good mechanical properties such as high resistance to the corrosion, very high strength to density ratio, faster installation and reduced maintenance costs (Obaidat et al., 2010); (El Gamal et al., 2019).

¹ **Corresponding author:**

Thi-Qar University – Nasiriya, IRAQ

E-mail: mamashrei@utq.edu.iq



(Barros et al., 2007); (El Gamal et al., 2019) presented that the strengthening of RC beams by CFRP using near-surface mounted (NSM) and externally bonded reinforcement (EBR) techniques have been increased the load-carrying capacity of RC beams by up to 114%, approximately, the same conclusion has been adapted by (Attari et al., 2012); (Khalifa, 2016) showed that the strengthening of RC beams by CFRP using NSM method has many advantages compared to the EBR method, such as reducing the risk of debonding, and much better protection from the external sources of damage. He found that the beams strengthened with NSM laminate achieved a higher maximum load than those strengthened with EBR for a similar area of CFRP. (Hong et al., 2011) and (El-Hacha and Rizkalla, 2004) found that the failure mode of RC beams strengthened by CFRP strips usually occurs due to CFRP strip rupture, accompanied by concrete compression failure. However, 65–75% of strips do not completely fracture. (De Lorenzis et al., 2000) studied the effect of groove size on the structural behavior of CFRP beams. An increasing groove size led to higher bond strength was observed. The maximum load increased by 8% and 24% as the groove size increased from 5/8 in. to 3/4 in.

(Hassan and Rizkalla, 2004) found that CFRP strips are better than CFRP rods in the strengthening of RC beams with NSM techniques with the same axial stiffness because the strips give a higher bond strength. (Hassan and Rizkalla, 2003) presented an experimental study to strengthen RC beams with NSM and they showed that the minimum clear spacing between the strips groove must not be less than twice the bar diameter. Also, the minimum edge distance should not be less than four times the bar diameter. (Lee et al., 2011) showed that the CFRP composite was used as external strengthened and as a cathodic protection (CP) system of steel in concrete elements. (Zaki and Rasheed, 2020) showed that the CFRP sheets used with both anchorage devices significantly increased the flexural capacity beyond that of unanchored and U-wrap anchored specimens. (Almusallam et al., 2018) showed that the ultimate capacity of the RC beams with opening not influenced by the opening in the pure flexural zone if the depth of the top chord was equal or greater than the depth of the concrete stress block. (Ghaedi et al., 2018) found that the CFRP with orthotropic or isotropic properties has no important influence on beam responses like stresses, displacements and damage response under applied loadings. Zhang et al., 2016) presented the finite element method (FEM) model to show the effects of localized cracks on the response of CFRP sheets used to strengthen RC beam. They concluded that FEM can be used to simulate crack propagation in structures under simple conditions.

Most of the previous works related to the strengthening of concrete beams by CFRP to enhance the flexure behavior of RC beams were experimental studies. It is very essential to understand the behavior of CFRP-RC beams by presenting more of theoretical and numerical studies. The theoretical works related to the behavior of RC beams with CFRP in flexure using program ABAQUS is still limited.

The purpose of this study to evaluate the accuracy of the finite element method (FEM) to represent RC beams retrofitted by CFRP under flexural loading. The results are compared with the experimental and ACI-440 results. The load-deflection relationship, crack pattern, strain in the concrete at the mid-span section of the beam and failure mode of all tested beams are studied. After validation of the FEM model, parametric studies are presented to assess the effect of the compressive strength of concrete, thickness, length of CFRP, and the presence of CFRP on the flexural strength of RC beams strengthened with CFRP.

2. Material properties

The same properties of steel reinforcement and concrete proposed by (Barros et al., 2007) have been used in this study. (Table 1) shows the properties of steel and concrete materials.

Two types of CFRP were used in this study: the first type is CFRP-sheets with 80 mm in width. The second type is CFRP-laminates with 1.4 x 9.6 mm² as a cross-sectional area. The properties of two types of CFRP are listed in the (Table 2).

Table 1. Properties of steel bars and concrete (Barros et al., 2017).

concrete f'_c (MPa)	steel		
	ϕ_s (mm)	(MPa) _{yf}	_{uf} (MPa)
52.2	5	788	890
	6.5	627	765
	6 (stirrups)	540	694



Table 2. Properties of the CFRP and adhesive materials (Barros et al., 2017).

CFRP type	Material	Tensile strength (MPa)	Young's modulus (GPa)	Ultimate strain (%)	Thickness (mm)
Sheet	primer	12	0.7	3	----
	epoxy	54	3	2.5	----
	CFRP	3700	240	1.5	0.111
Laminate	Adhesive	16-22	5	----	----
	CFRP	2740	158.8	1.7	1.4

3. Finite element analysis

Nonlinear finite element analysis was performed to study the behavior of RC beams. ABAQUS program was used in this study.

3.1 Concrete

Plastic damage was performed to represent concrete. The main failure modes of the concrete are tensile cracking and compression failure as shown in (Figure 1) (Hibbit and Sorensen, 2000). The modulus of elasticity (E_c) and modulus of rupture was calculated theoretically based on experimental values of the compressive strength of concrete (f'_c) using (Equation 1) and (Equation 2) (European Committee for Standardization, 2004) (ACI, 2019). Also, the stress-strain curve of concrete in the tension and compression behavior in the plastic zone was calculated from (Equation 3); (Equation 4); (Equation 5); (Equation 6); (Equation 7); (Equation 8) and (Equation 9) (European Committee for Standardization, 2004).

For tension behavior:

$$f_t = 0.61 \sqrt{f'_c} \quad (1)$$

$$E_c = 22 (0.1 * f'_c)^{0.3} 1000 \quad (2)$$

$$\epsilon = 0.000117$$

$$\epsilon_{ct} = \epsilon_t = F_t / E_c \quad (3)$$

$$\sigma_t = f_t (\epsilon_t / \epsilon)^{0.4} \quad (4)$$

$$\epsilon_{cst} = \epsilon_t - \left(\frac{\sigma}{E_c} \right) \quad (5)$$

For compressive behavior:

$$k = 1.05 * E_c \left(\frac{\epsilon_{c1}}{f'_c} \right) \quad (6)$$

$$\epsilon_{c1} = 0.0014 (2 - e^{0.024 * f'_c} - e^{0.14 f'_c}) \quad (7)$$



$$\kappa = \epsilon_c / \epsilon_{c1} \quad (8)$$

$$\sigma_c = f'_c * \left(\frac{k * \kappa - \kappa^2}{1 + (k-2) * \kappa} \right) \quad (9)$$

where:

f_t : tensile strength of concrete, f'_c : compressive strength of concrete, E_c : elastic modulus, ϵ_t : strain in the tension zone, σ_t : tensile stress in plastic range, ϵ_{cst} : tensile strain in the plastic range, ϵ_{c1} : strain at the peak stress, σ_c : compressive strength of concrete in plastic range.

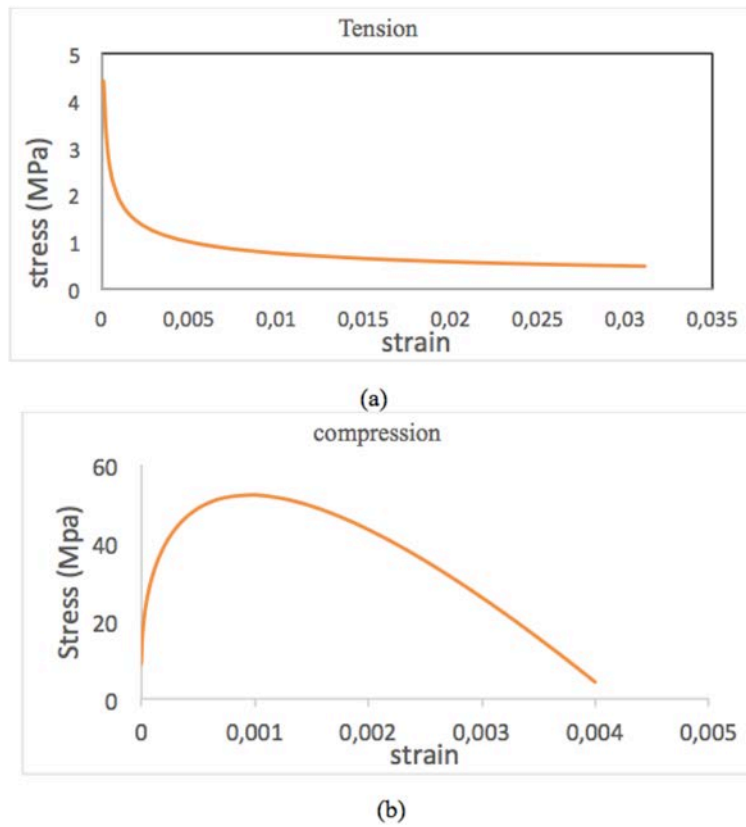


Figure 1. Stress-strain curves of concrete: a) tensión b)compression (European Committee for Standardization, 2004).

3.2 Steel reinforcement

The steel reinforcement was used as an elastic-plastic material according to CEN, Eurocode, design of steel structures-Part 1-1: General rules and rules for buildings (CEN, 2005). (Figure 2) shows the stress-strain relationship of steel in compression and tension behavior. The modulus of elasticity and the yield stress of steel bars were obtained from the experimental work conducted by (Barros et al, 2007). A Poisson's ratio of 0.3 was used in this study. A perfect bond between concrete and steel was assumed.



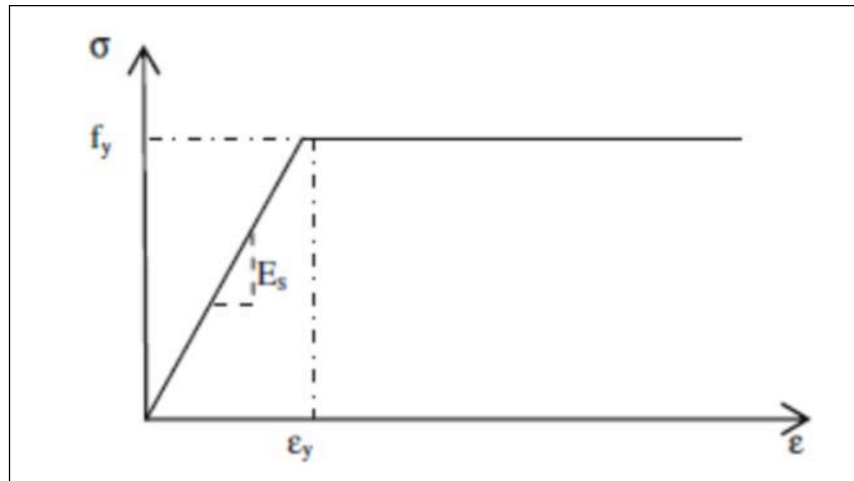


Figure 2. "Stress-strain relationship of steel bar in tension and compression (CEN, 2005)".

3.3 CFRP

Generally, two models were used to represent CFRP. Firstly, CFRP was assumed as a linear elastic isotropic until failure. While in another model, CFRP was assumed as a linear elastic orthotropic material. The first model has been used in this study. The CFRP properties as specified by the manufacturer. A Poisson's ratio of 0.3 was used for CFRP. The stress-strain of CFRP is shown in (Figure 3).

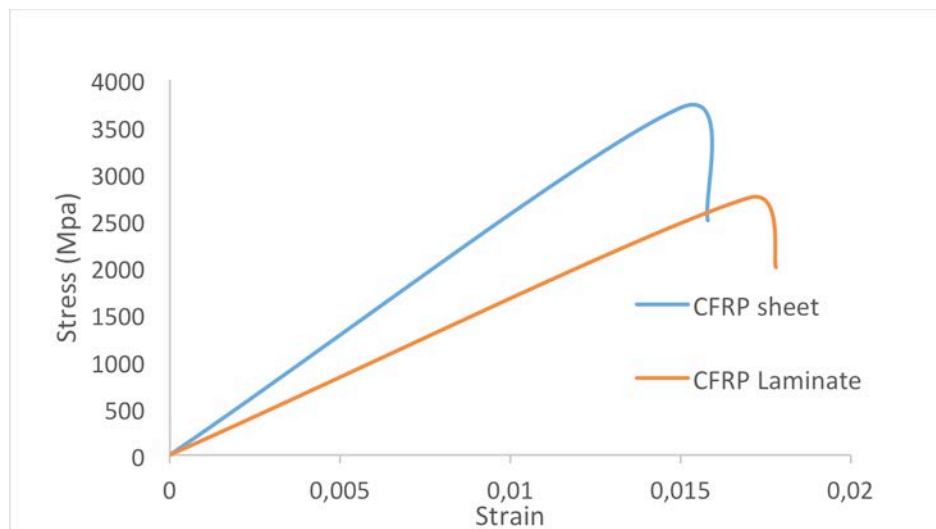


Figure 3. Stress-strain curve of CFRP for sheet and laminate.

3.4 CFRP–concrete interface

Two models were utilized to model the interface between CFRP concrete surfaces. A perfect bond was assumed in the first model and a cohesive model was assumed in the second one. (Figure 4) shows the relationship between maximum shear stress (τ_{max}) and effective opening displacement (δ) in the interface zone between concrete and CFRP by using simple bilinear traction–separation law. The interface is modeled with a small thickness and the initial stiffness K_0 is defined as shown in (Equation 10) (Guo et al., 2005):

$$K_0 = \frac{1}{\frac{t_i}{G_i} + \frac{t_c}{G_c}} \quad (10)$$



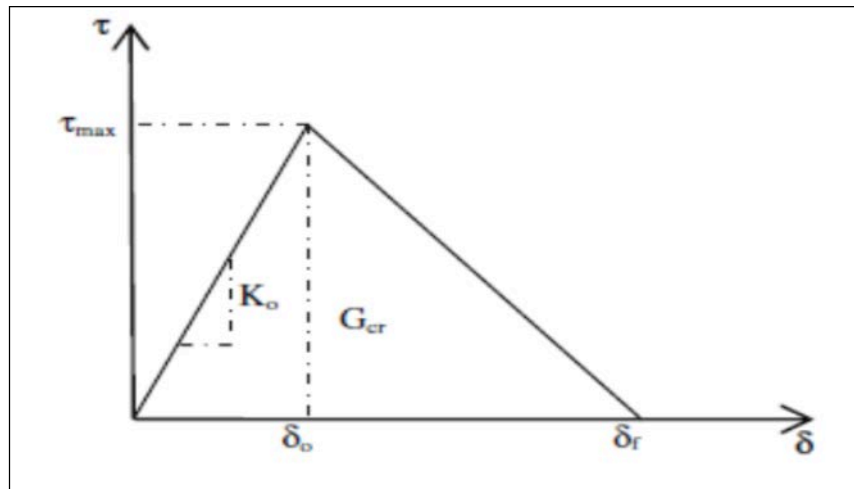


Figure 4. Bilinear traction–separation constitutive law.

It is assumed that $G_i = 0.665 \text{ GPa}$, $G_c = 10.8 \text{ GPa}$, $t_i = 0.5 \text{ mm}$, and $t_c = 5 \text{ mm}$. The relation between the effective opening displacement and traction stress is represented by the stiffness (K_o), opening displacement at fracture (δ_r), the material strength (τ_{max}) and the energy required to open the crack (G_{cr}) which is defined by the area under the traction–displacement relationship as shown in (Figure 4). (Equation 11) and (Equation 12), (Lu et al., 2005), gives the maximum value of shear stress (t_{max}):

$$t_{max} = 1.5 Bw f_t \quad (11)$$

$$Bw = \sqrt{\frac{2.25 - \frac{bf}{bc}}{1.25 + \frac{bf}{bc}}} \quad (12)$$

where:

The value of fracture energy (G_{cr}) was ranged between 300 J/m^2 and 1500 J/m^2 as assumed by others (JCI, 2003) (JCI, 1998). The value of 900 J/m^2 was used in current research.

The damage was assumed to occur firstly when the nominal stress ratios reached the value one, this criterion can be represented by (Equation 13) (Hibbitt and Sorensen, 2000):

$$(\sigma_n / \sigma_n^o)^2 + (t_s / t_s^o)^2 + t_t / t_t^o)^2 = 1 \quad (13)$$

$\sigma_n^o = f_t = 4.4 \text{ MPa}$, and $t_s^o = t_t^o = 1.5 \text{ MPa}$, used for this study.

4. Structural modeling using ABAQUS

Generally, each analytical model using the ABAQUS program will be processed in the following steps:

1. Build up the geometry of the structure under a set of elements. (part module, mesh module).

In this study, the part module consists of the concrete beam, CFRP sheet or laminate, and reinforcing steel. While the meshing process based on different factors, such as the geometric specifications. Generally, the meshing process is straightforward. The process consisted of two stages. In the first stage, seeds are assigned to the edge of the components and in the second stage, meshes are assigned to each part. The desired level of accuracy depends on the size of the mesh.

2. produce element sections (property module)



The property module contains the input of the nonlinear stress-strain curves of material for each part.

3. Introduce material information (property module)
4. Assign material properties and section to the members (Property module)
5. Assemble parts to make the complete structure (assembly module, mesh module, and interaction module).

Models usually consist of the components that are assembled to form the final shape. These components are known as part instances. For example, the model in this study consisted of CFRP laminates or sheet concrete, steel rods, and epoxy layers. It is more convenient to model each of these elements separately and then assemble them. This method is considerably helpful for forming complex configurations.

6. Create steps and select analysis method (step module)
7. Introduce boundary conditions and load (load module)

In this study, simply supported beams subjected to four-point load have been modeled.

8. Work jobs and submit for analysis (job module)
9. Visualize the result. (visualization module). The results showed by figures and tables.

5. Flexural strengthening

Numerical modeling of the structural behavior of RC beams strengthened by CFRP under four-point bending was presented. The experimental work conducted by (Barros et al., 2007).

(Table 3) and (Figure 5) show the reinforcement arrangements, the geometry of the beams type, the number and position of the CFRP strengthened systems. FEM was used to study the flexural behavior of RC beams using the ABAQUS program, a flowchart showing the research methodology was presented in (Figure 6).

Table 3. Beam series for the flexural strengthening.

Beam designation	Type of strengthening	CFRP type	Number of sheet Layer/laminate strip
S1-R	-	-	-
S2-R	-	-	-
S3-R	-	-	-
S1-EXT-LAM	external	CFRP laminate	1
S2-EXT-LAM	external	CFRP laminate	2
S3-EXT-LAM	external	CFRP laminate	3
S1-NSM	NSM	CFRP laminate	1
S2-NSM	NSM	CFRP laminate	2
S3-NSM	NSM	CFRP laminate	3
S1-EXT-M	external	CFRP sheet	1
S2-EXT-M	external	CFRP sheet	2
S3-EXT-M	external	CFRP sheet	3



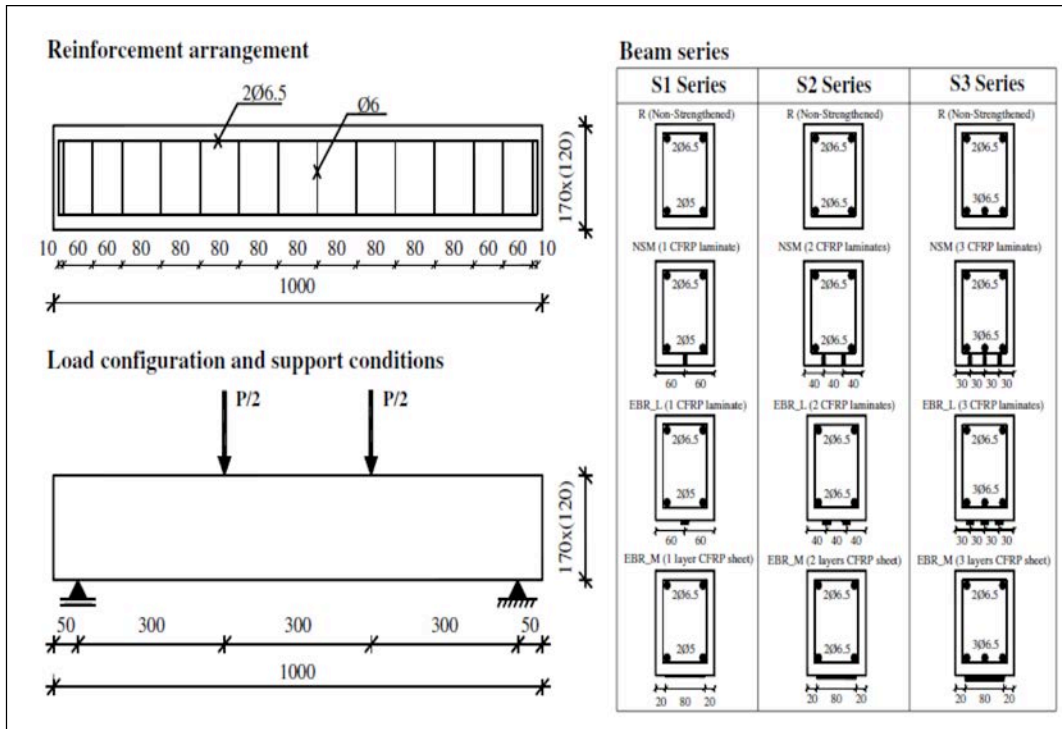


Figure 5. Beam series for the flexural strengthening (dimension in mm) (Barros et al., 2007).

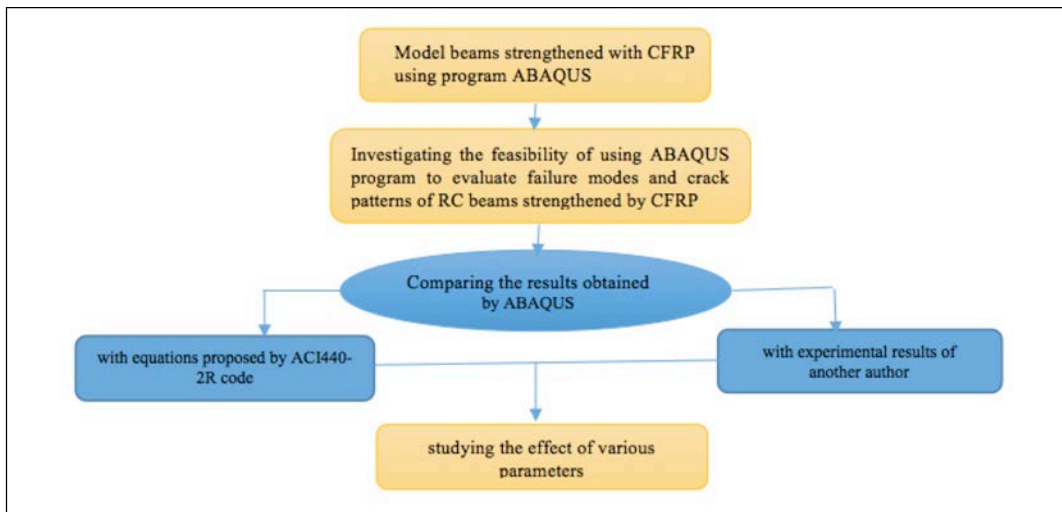


Figure 6. A flowchart showing the research methodology.

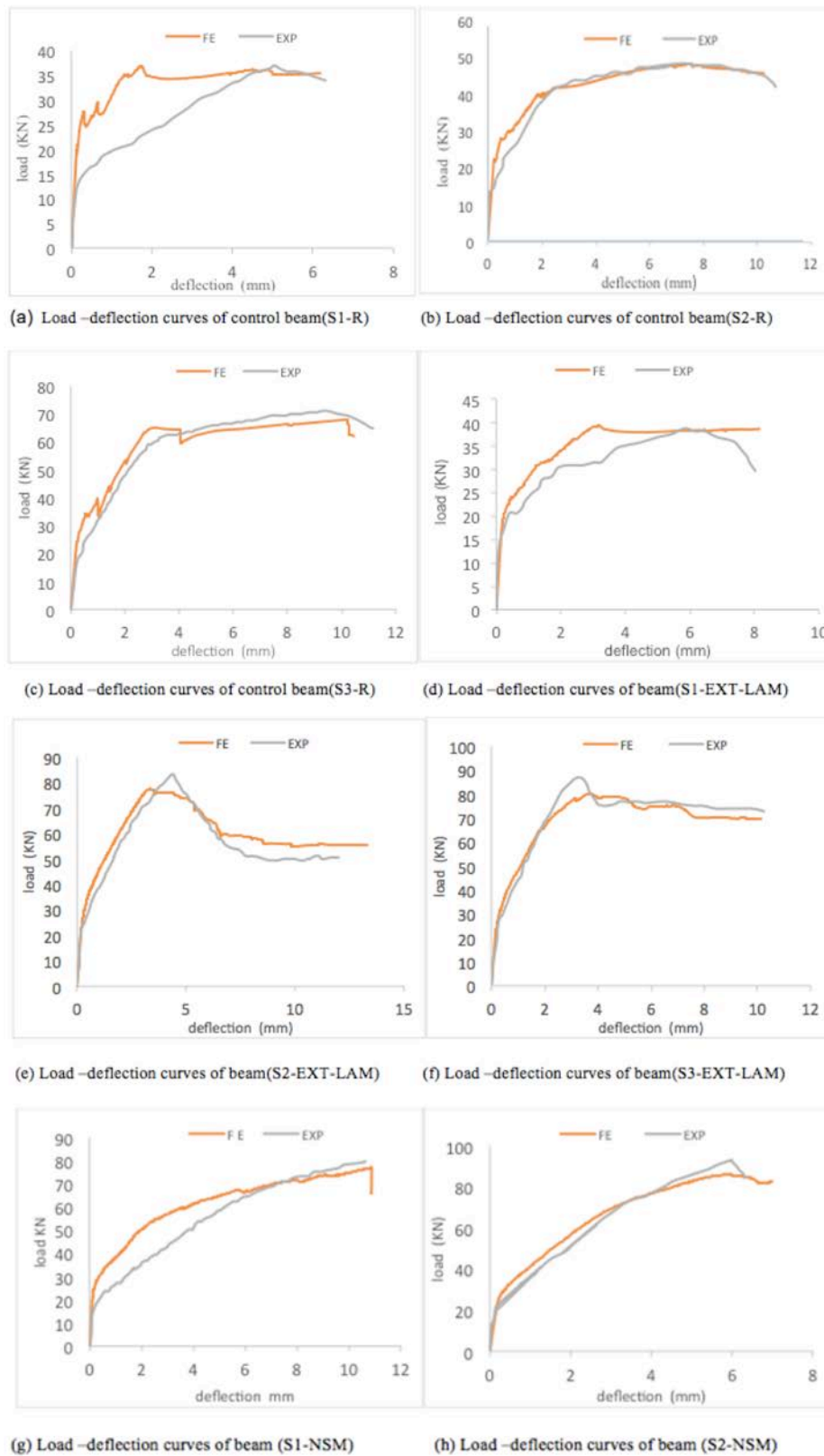
6. Results and discussion

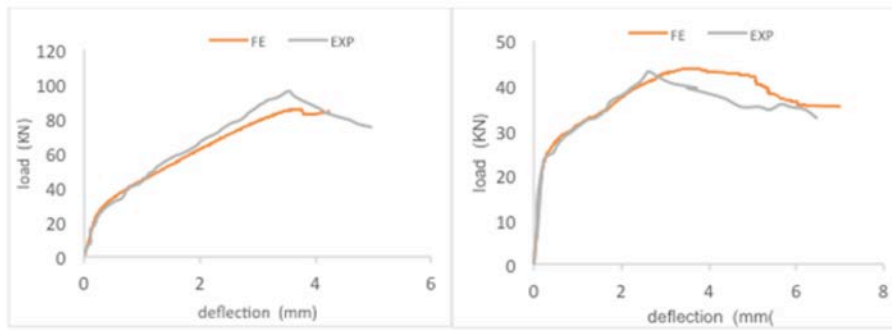
6.1 Load-deflection curve

The control beams S1-R, S2-R, and S3-R failed at loads of 36.9, 47.84 and 67.94 kN respectively. While, the strengthened beams S1-EXT-LAM, S2-EXT-LAM, S3-EXT-LAM, S1-NSM, S2-NSM, S3-NSM, S1-EXT-M, S2-EXT-M, and S3-EXT-M were failed at loads of 39.34, 77.33, 80.17, 77.05, 86.12, 86.31, 43.72, 84.38 and 89.76 kN respectively. It should be noted that the load-carrying capacities of strengthened beams: S1-EXT-LAM, S2-EXT-LAM, S3-EXT-LAM, S1-NSM, S2-NSM, S3-NSM, S1-EXT-M, S2-EXT-M, and S3-EXT-M have been increased by 6.6%, 61.6%, 18%, 108.8, 79.96%, 26%, 18.4%, 76.3%, 32.1% respectively when compared with the load-carrying capacity of control beam(S1-R). The maximum gain in the strength was obtained when the RC beam strengthened by NSM, (Table 4) also, shows the percentage of increase for all beams. Also, the results showed that when increasing



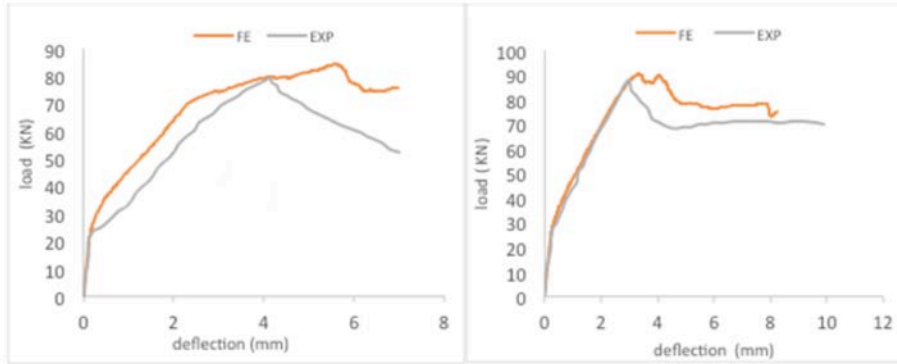
the amount of CFRP by 50% the load-carrying capacity increased only by 3.6%, this is very clear when comparing the load-carrying capacity of the beam S3-EXT-LAM with the beam S2-EXT-LAM. This means that the increase at a certain limit of the amount of CFRP may be led to a slight increase in the maximum load. The load- midspan deflection curves for the control and strengthened beams are shown in (Figure 7). It is clear from this figure there is a good agreement between the experimental and FE results. (Table 4) shows experimental and FE results.





(i) Load-deflection curves of the beam (S3-NSM)

(j) Load-deflection curves of the beam(S1-EXT-M)



(k) Load –deflection curves of beam(S2-EXT-M)

(m) Load –deflection curves of beam(S3-EXT)

Figure 7. Load-deflection curves of beams strengthened for flexure.

Table 4. Finite element and experimental results.

Beam designation	Experimental(EXP) [1]		Finite element method (FE)			Pmax_EXP /Pmax_FE	Pser_EXP /Pser_FE
	Pmax_EXP (KN)	Pser_EXP* (KN)	Pmax_FE (KN)	Percentage Increase in Capacity (%)	Pser_FE** (KN)		
S1-R	36.6	22.1	36.90	---	34.33	0.99	0.64
S2-R	48.5	40.5	47.84	---	41.68	1.01	0.97
S3-R	71.8	51.5	67.94	---	56.2	1.05	0.91
S1-EXT-LAM	38.6	31.9	39.34	6.6	35.62	0.98	0.89
S2-EXT-LAM	83.5	57.6	77.33	61.6	64.90	1.07	0.88
S3-EXT-LAM	86.5	74.1	80.17	18.0	70.12	1.07	1.05
S1-NSM	79.9	37.5	77.05	108.8	52.42	1.03	0.71
S2-NSM	93.3	56.3	86.12	80.0	60.73	1.03	0.92
S3-NSM	96.6	71.5	86.31	27.0	66.53	1.12	1.07
S1-EXT-M	43	40.3	43.72	18.4	39.02	0.98	1.03
S2-EXT-M	79.5	59.5	84.38	76.3	68.96	0.94	0.86
S3-EXT-M	87.3	73.4	89.76	32.1	74.85	0.97	0.98

* The experimental load at a deflection of L/400

** The FEM load at a deflection of L/400



6.2 Modes of Failure

The control beams failed by yielding of main reinforcement. The flexural cracks formed followed a typical flexure crack. The first visible crack was observed in the flexural region. New cracks started to form when the load was increasing as shown in (Figure 8). Beams (S1-EXT-LAM, S2-EXT-LAM, and S3-EXT-LAM) failed by debonding of CFRP strip. The debonding was followed by the crushing of concrete. The debonding started from end-span due to the intermediate crack mechanism typically after yielding of primary steel reinforcement when the flexural cracks widen as shown in (Figure 9). In beam S1-NSM, the failure occurred after yielding of steel reinforcement and CFRP strips rupture, this failure usually takes place in lightly reinforced and lightly strengthened sections while beams S2-NSM and S3-NSM failed by yielding of main reinforcement and then concrete cover separation has occurred as shown in (Figure 10). This failure starts at the CFRP curtailment because of stress concentration at the plate or sheet. Once cracking starts at an angle and then changes to a horizontal crack parallel to steel bar at the level of major steel because the stirrups reinforcement work to hold the inclined crack. The fracture of the CFRP sheet in two pieces has occurred in beam S1-EXT-M, the flexural strength of the beam dropped gradually while beams S2-EXT-M and S3-EXT-M failed by concrete cover separation as shown in (Figure 11). The failure mode of beam S2-EXT-M is different from the experimental failure mode. Numerically the beam (S2-EXT-M) failed by concrete cover separation while experimentally the failure was by rupture of CFRP. Also, the failure mode of S1-NSM is different from experimental failure. Numerically the beam failed by rupture of CFRP while experimentally the beam failed by yielding of the longitudinal reinforcement and then concrete cover separation has occurred.

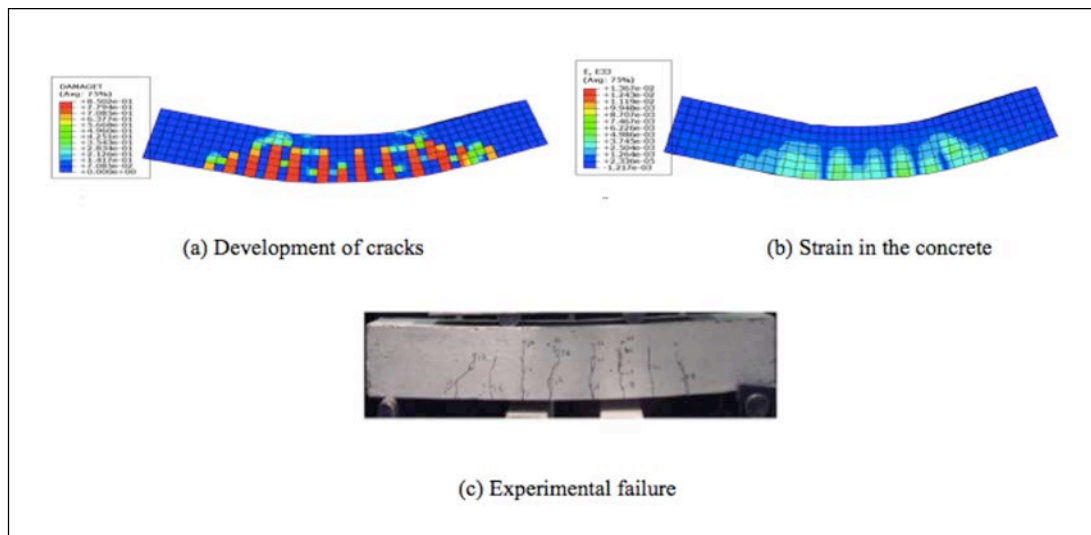


Figure 8. The typical failure modes of control beams: (a) development of cracks, (b) strain in concrete, and (c) experimental failure.

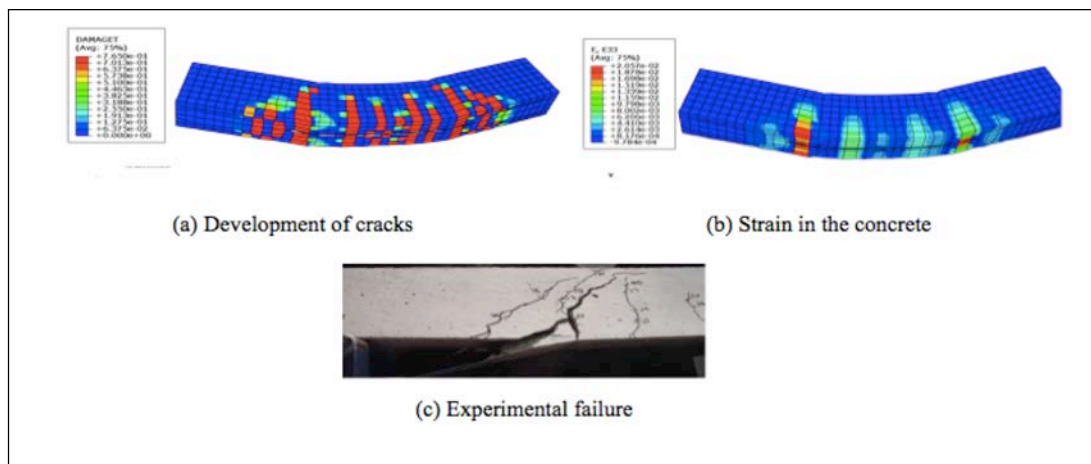


Figure 9. The typical failure modes of beams strengthened with CFRP-EBR stripe a) development of cracks, b) strain in the concrete and c) experimental failure.

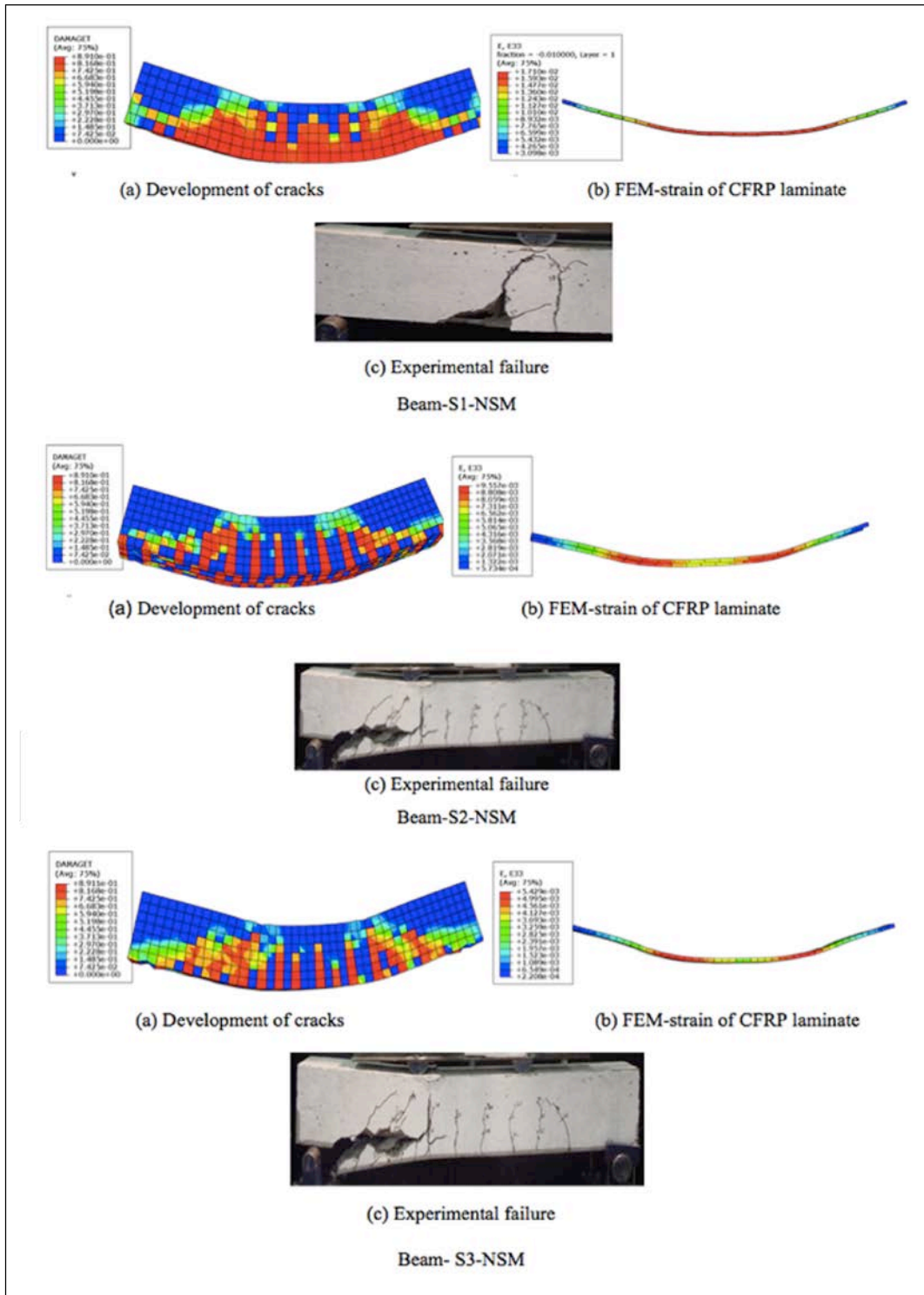


Figure 10. The typical failure modes of RC beams (S1-NSM, S2-NSM and S3-NSM) strengthened CFRP strip using NSM method.



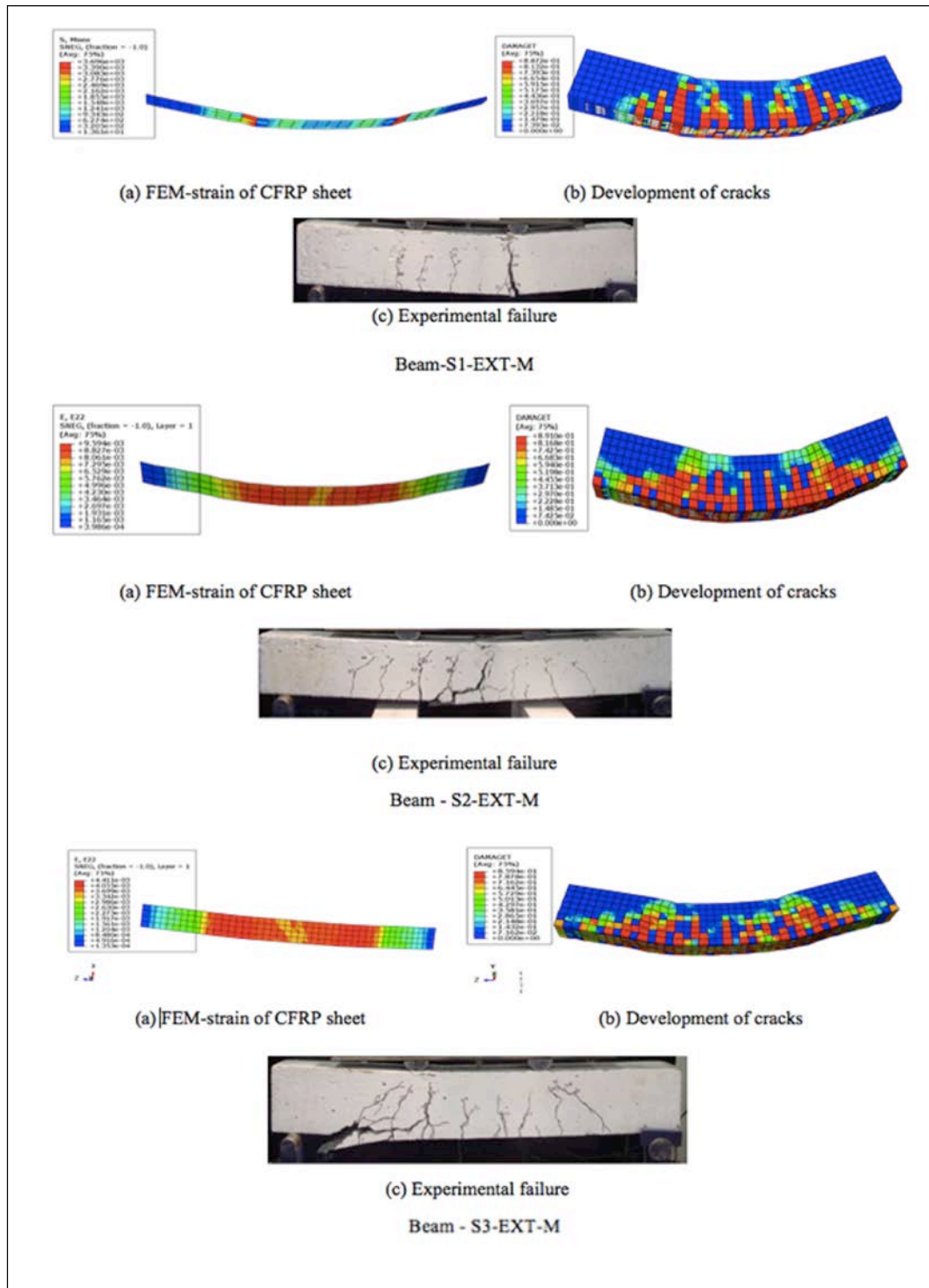


Figure 11. The typical failure modes of RC beams (S1-EXT-M, S2-EXT-M and S3-EXT-M) strengthened by external sheets.



6.3 Parametric study

6.3.1 Effect of compressive strength of concrete

The strength of concrete (f'_c) is an important parameter related to the behavior of RC beams. Five different concrete compressive strength (30 MPa, 40 MPa, 52.2 MPa, 60 MPa, and 70 MPa) were considered to assess the effect of f'_c on the behavior of CFRP-RC beams. (Figure 12) shows the effect of f'_c on the behavior of EBR and NSM beams. It seems that the maximum load and stiffness increased with increases in the compressive strength while the maximum deflection decreased with increases in the compressive strength for concrete. (Figure 13) explains the relationship between compressive strength and maximum load. Mode of failure changed from rupture of CFRP stirrups to delamination of the concrete cover in near-surface mount techniques at $f'_c = 30$ MPa, while, in other beams, no change in the mode of failure has occurred.

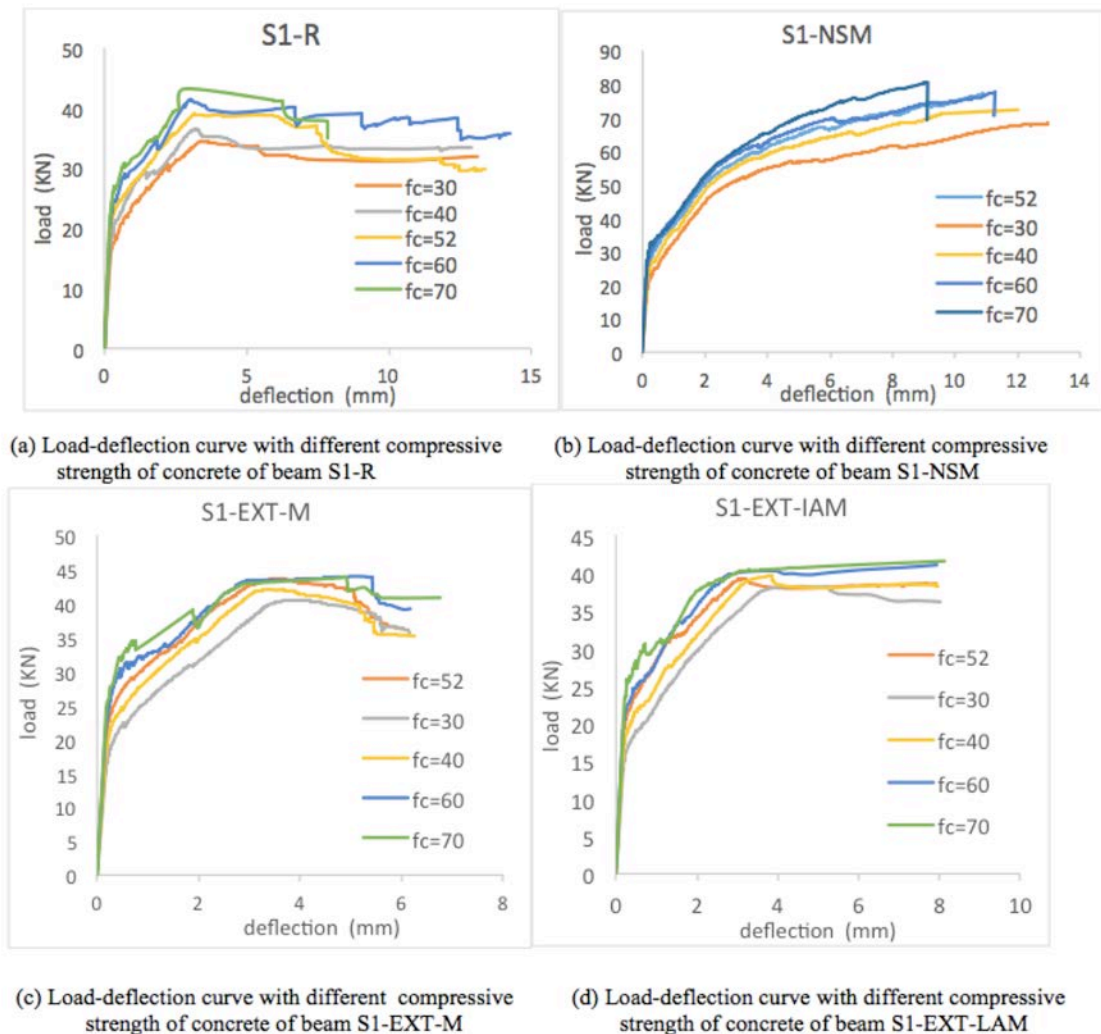


Figure 12. Load-deflection curves with different compressive strength of concrete.



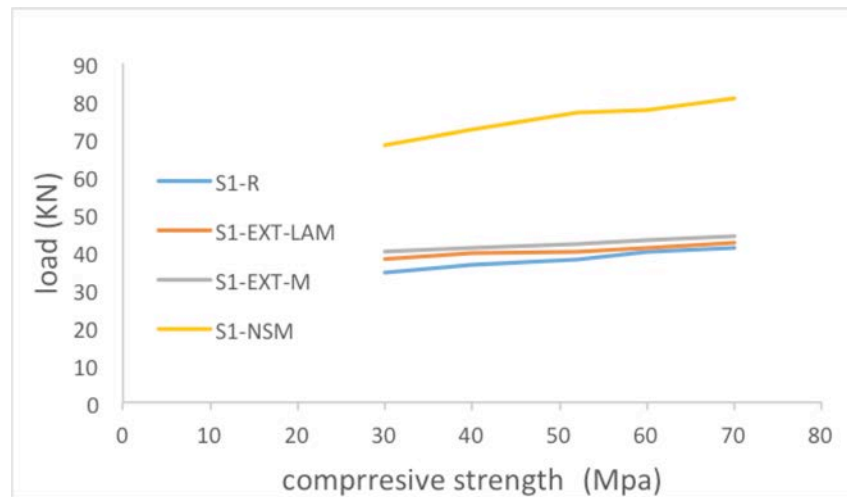
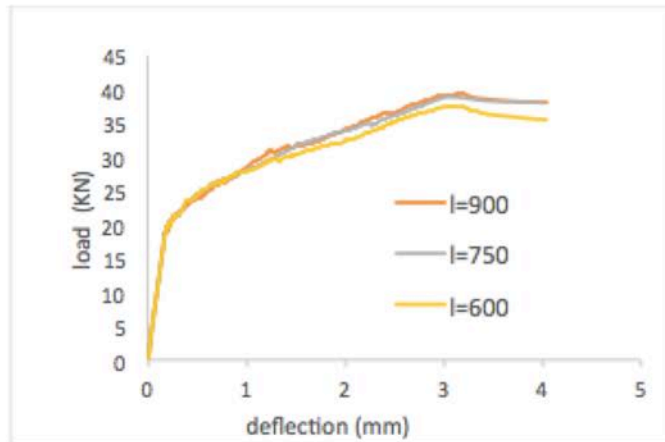


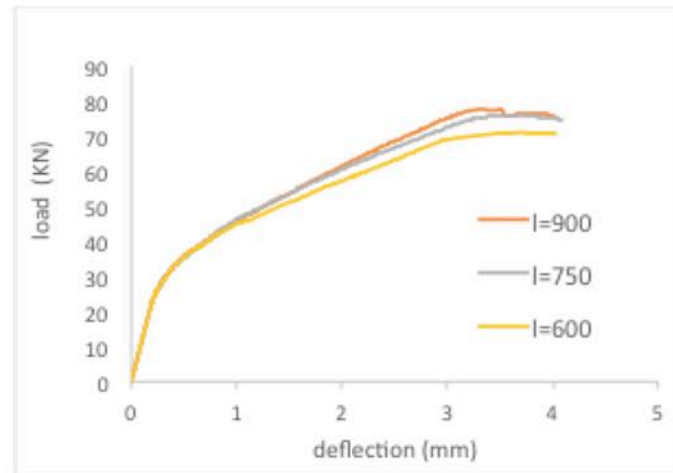
Figure 13. Effect of compressive strength on the maximum load.

6.3.2 Effect of length of CFRP laminate

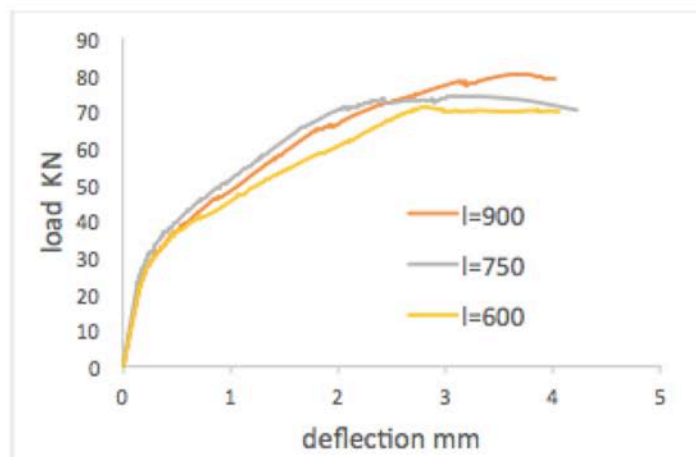
The efficiency of the strengthening RC beam by CFRP depends on the length of the CFRP laminate. Three different values of length of CFRP laminate ($L=900$, $L=750$, and $L=600$) mm have been used to study the effect of the length on the behavior of RC beams strengthened with CFRP. (Figure 14) shows that the stiffness of all beams at a load equal to 20 kN is almost the same, after that the strengthened beam with a length of CFRP equal to 900 mm is more stiffness than the beam with length equal to 600 mm. This may be attributed to the beam strengthened with length equal to 900 mm of CFRP laminate have a sufficient length outside the region of the maximum moment and it is more efficient in the critical zone. The debonding failure has been occurred in all beams due to high shear stress at the end of the CFRP laminate. However, the properties of the epoxy are important concerning the debonding failure. Also, from this figure can be seen that the maximum load of beam strengthened with a length of CFRP 900 mm higher than a load of beams with a length of 600 mm and 750 mm as shown in (Figure 15). Finally, it can be observed that the length of CFRP has an important effect on the stiffness as well as on the strength of RC beams.



(a) Load-deflection curve for beam (S1-EXT-LAM) Strengthened by different length of CFRP laminate



(b) Load-deflection curve for beam (S2-EXT-LAM) Strengthened by different length of CFRP laminate



(c) Load-deflection curve for beam (S3-EXT-LAM) strengthened by different length of CFRP laminate

Figure 14. Load-deflection curve of strengthened beams with different length of CFRP.



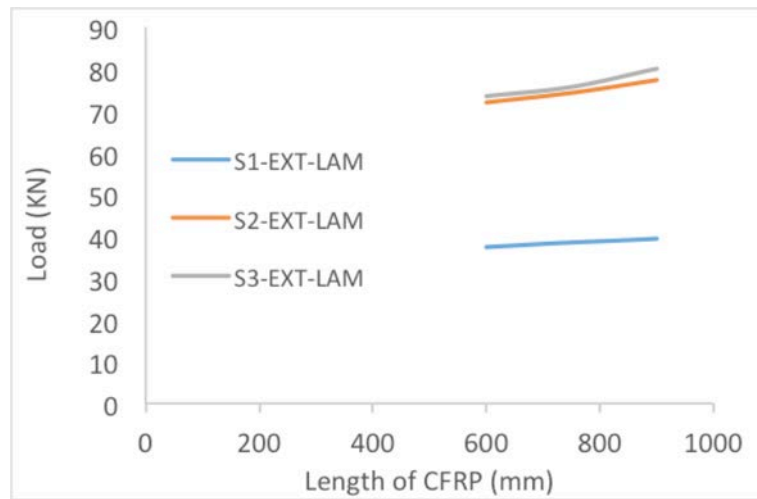
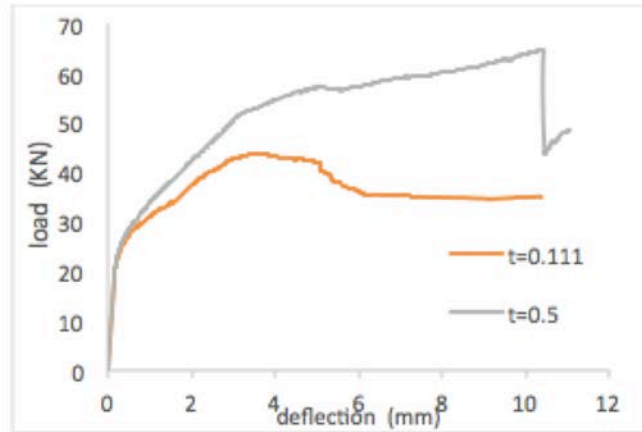


Figure 15. Effect of length of CFRP on the maximum load.

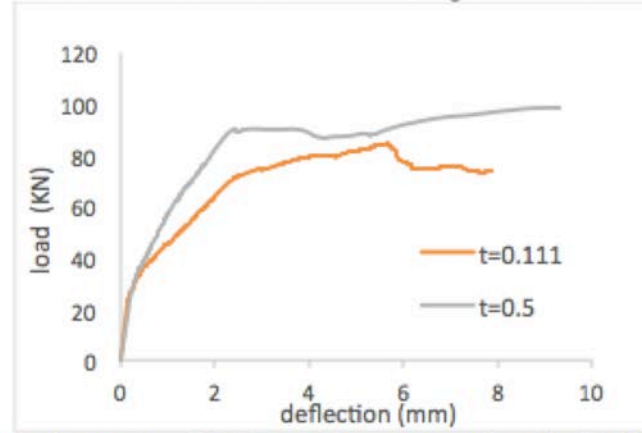
6.3.3 Effect of thickness of CFRP sheet

Three beams (*S1-EXT-M*, *S2-EXT-M*, and *S3-EXT-M*) have been used as a case study to investigate the effect of CFRP sheet thickness on the behavior of CFRP- RC beams. Two values of thickness were used (0.5 and 0.111 mm). (Figure 16) shows that the increase of thickness of the CFRP sheet leads to an increase in the stiffness and max load of the beams due to increasing the cross-section of CFRP. Also, (Figure 17) shows the relationship between the max load and the thickness of the CFRP sheet.

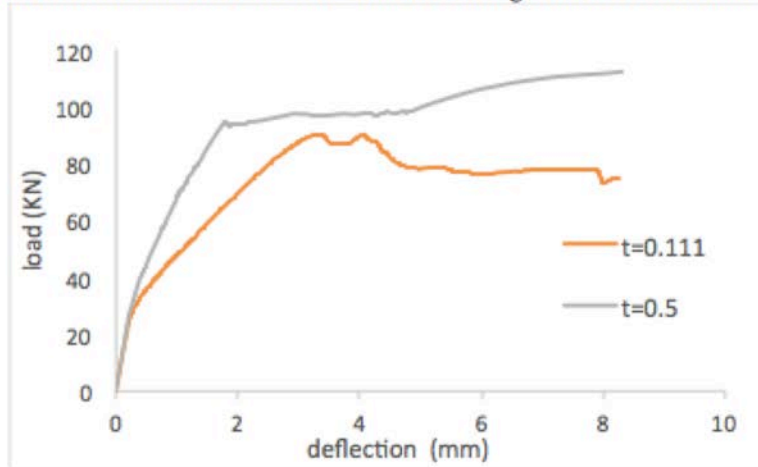




(a) load-deflection curves of S1-EXT-M beams strengthened with different thickness of CFRP



(b) load-deflection curves of S2-EXT-M beams strengthened with different thickness of CFRP



(c) load-deflection curves of S3-EXT-M beams strengthened with different thickness of CFRP

Figure 16. load-deflection curves of RC beams Strengthened with different thickness of CFRP.



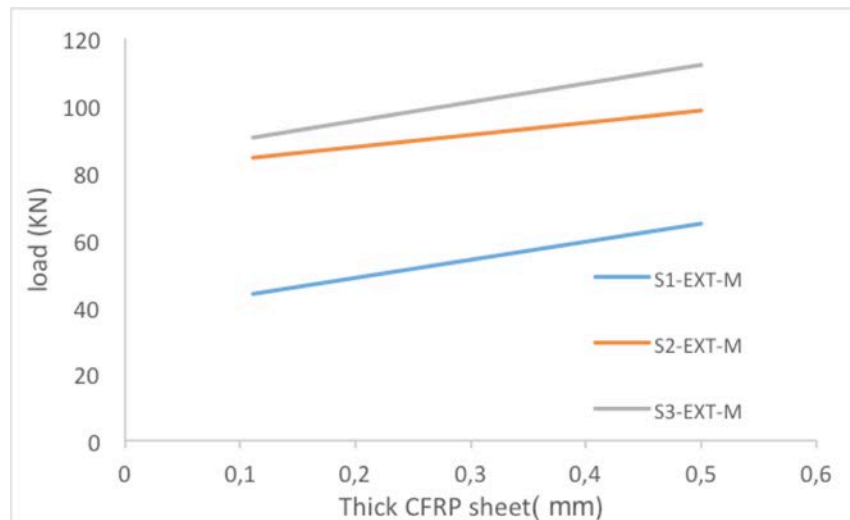


Figure 17. Relationship between maximum load and thickness of CFRP sheet.

6.3.4 The effect of the presence of CFRP on steel bar stresses

In this study, four beams (S2-EXT-M, S2-NSM, S2-EXT-LAM, and S2-R) have been used to investigate the effect of the presence of CFRP on steel bar stresses. (Figure 18) shows that the load at yield point of steel reinforcement in S2-R, S2-NSM, S2-EXT-LAM, and S2-EXT-M beams was 46.2, 72.5, 74.3 and 78.1 respectively. This indicated that the presence of CFRP has an effect on the applied load at the yielding of steel regardless of the type of strengthening. This means that the CFRP has a contribution to carrying the applied load.

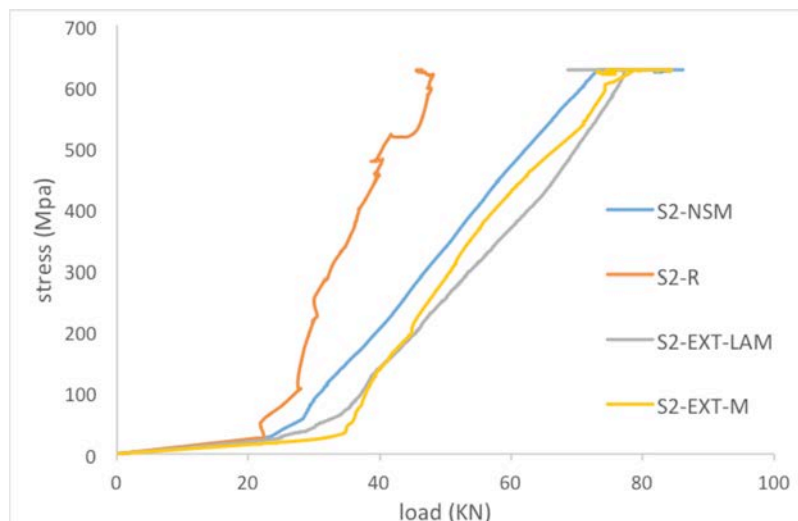


Figure 18. Relationship between stresses in steel bar and max load in beam.

6.3.5 The strain distribution through the depth of control and strengthened beams

The finite element model with an effective depth of 300 mm was developed to show the strain distribution through the depth of the beams. (Figure 19) shows the strain distribution of beams (S2-R, S2-NSM, S2-EXT-LAM, and S2-EXT-M), it is clear that the beams with CFRP sheet or laminate have more strain in compression and tension zone than the control beam (S2-R).



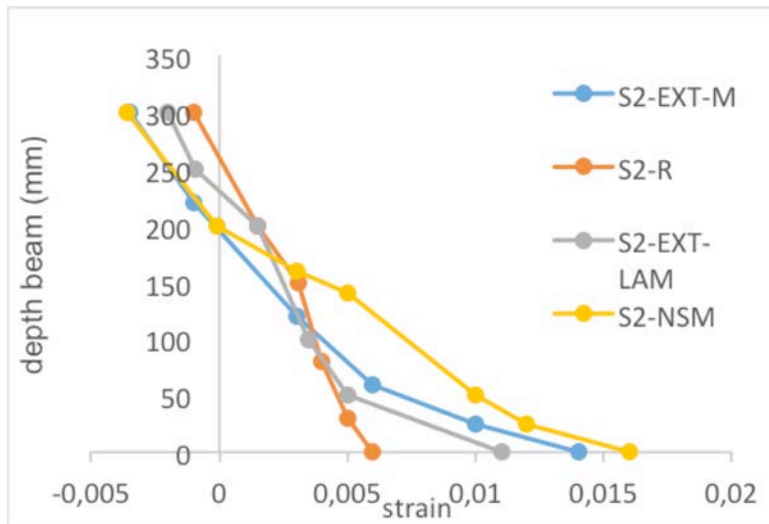


Figure 19. Strain distribution of concrete through the depth of beams.

6.4 Appraisal of the ACI-440

The ultimate load of externally bonded reinforcement (EBR) beams can be calculated by ACI-440 (Equation 14) and (Equation 15) as follow:

$$M = A_{s1} * F_{syd}(d_s - 0.4 * x) + \gamma_f * A_f * F_{fe}(h - 0.4x) \quad (14)$$

Where:

$$F_{fe} = E_{fe} * F_e \quad (15)$$

(Table 5) shows the results of the FE method and ACI equation for RC beams for flexure behavior, from this table it can be concluded that the ACI equation is underestimated.

Table 5. Results of finite element method (FEM) and ACI equation.

Beam designation	Maximum load (KN)		FEM/ACI
	FEM	ACI	
S1-EXT-LAM	39.34	45.3	0.87
S2-EXT-LAM	77.33	70.4	1.10
S3-EXT-LAM	80.17	103.8	0.77
S1-NSM	77.05	62.8	1.22
S2-NSM	86.09	99.2	0.87
S3-NSM	85.6	136.7	0.63
S1-EXT-M	43.72	60.8	0.72
S2-EXT-M	84.38	100.5	0.84
S3-EXT-M	89.76	143.5	0.63



7. Conclusions

1. In general, the finite element method was presented in this research to investigate the behavior of RC beams strengthened by CFRP sheet or laminate using ABAQUS application. The results were indicated that a good agreement with the available experimental results. The maximum difference between the load-carrying capacity of numerical and experimental results was 12%.
2. The results indicated that the strengthening of RC beams by the CFRP system improves the strength of the RC beams by up to 108.8%.
3. Increasing the compressive strength of concrete (f_c') tends to increase the maximum load of strengthened RC beams. Increasing f_c' from 30 MPa to 70 MPa makes an increase in the strength of the beam to reach 25.6% as well as the stiffness of the beam was increased.
4. The increasing number of strips or the number of layers of the CFRP sheet tends to increase the strength of RC beams.
5. Increasing the length of CFRP from 600 mm to 900 mm leads to an increase in the strength by 12.7%.
6. Increasing thickness of CFRP sheet from 0.11 mm to 0.5 mm lead to an increase in the strength of the beam by 47.9%.

8. References

- ACI (2019). Building Code Requirements for Structural Concrete 2019, American Concrete Institute.
- Almusallam, T., et al. (2018). Behavior of FRP-Strengthened RC Beams with Large Rectangular Web Openings in Flexure Zones: Experimental and Numerical Study. *International Journal of Concrete Structures and Materials*. 12(1): p. 47.
- Attari, N.; Amziane, S.; Chemrouk, M. (2012). Flexural strengthening of concrete beams using CFRP, GFRP and hybrid FRP sheets. *Construction and Building Materials*. 37: p. 746-757. DOI: <https://doi.org/10.1016/j.conbuildmat.2012.07.052>.
- Barros, J.A.; Dias, S.J.; Lima, J.L. (2007). Efficacy of CFRP-based techniques for the flexural and shear strengthening of concrete beams. *Cement and Concrete Composites* 29(3): p. 203-217. DOI: <https://doi.org/10.1016/j.cemconcomp.2006.09.001>.
- Bodzak, P. (2019). Flexural behaviour of concrete beams reinforced with different grade steel and strengthened by CFRP strips. *Composites Part B: Engineering*. 167: p. 411-421. DOI: <https://doi.org/10.1016/j.compositesb.2019.02.056>.
- CEN (2005). Eurocode 3: Design of steel structures - Part 1-1: General rules and rules for buildings Brussels: CEN.
- De Lorenzis, L.; Nanni, A.; La Tegola, A. (2000). Strengthening of reinforced concrete structures with near surface mounted FRP rods. in *International Meeting on Composite Materials, PLAST 2000, Proceedings, Advancing with Composites*. DOI: https://www.academia.edu/download/48497838/Strengthening_of_Reinforced_Concrete_Str20160901-6048-n42m5.pdf.
- El Gamal, S., et al., (2019). Flexural behavior of RC beam strengthened with CFRP sheet using different strengthening techniques. *The Journal of Engineering Research [TJER]*. 16(1): p. 35-43. DOI: <http://dx.doi.org/10.24200/tjer.vol16iss1pp35-43>.
- El-Hacha, R.; Rizkalla, S.H. (2004). Near-surface-mounted fiber-reinforced polymer reinforcements for flexural strengthening of concrete structures. *Structural Journal*. 101(5): p. 717-726. DOI: <https://www.concrete.org/publications/internationalconcreteabstractsportal/m/details/id/13394>.
- European Committee for Standardization (2004). 1992-1-1, E., Design of concrete structures - Part 1-1: General rules and rules for buildings.
- Ghaedi, K. (2018). Finite element analysis of strengthened beam deliberating elastically isotropic and orthotropic CFRP materia. *Journal of Civil Engineering, Science and Technology*. 9(2):117-126 . DOI: <http://publisher.unimas.my/ojs/index.php/JCEST/article/view/991/651>.
- Guo, Z., et al. (2005). Experimental study on bond stress-slip behaviour between FRP sheets and concrete. in *FRP in construction, proceedings of the international symposium on bond behaviour of FRP in structures*. DOI: https://www.researchgate.net/profile/Serge_Shilko/post/how_to_study_slip_and_interface_effects_of_steel_confined_composite_beams_under_flexure/attachment/59d6280779197b807798662a/AS:328343963619331@1455294709660/download/Experimental+Study+on+Bond+Stress-Slip+Behaviour+between+FRP+Sheets+and+Concrete.pdf.
- Hassan, T.; Rizkalla, S. (2003). Investigation of bond in concrete structures strengthened with near surface mounted carbon fiber reinforced polymer strips. *Journal of composites for construction*. 7(3): p. 248-257. DOI: <http://citeseerx.ist.psu.edu/viewdoc/download?doi=10.1.1.493.4170&rep=rep1&type=pdf>.
- Hassan, T.; Rizkalla, S. (2004). Bond mechanism of NSM FRP bars for flexural strengthening of concrete structures. *ACI Structural Journal*. 101(6): p. 830-839. DOI: <http://citeseerx.ist.psu.edu/viewdoc/download?doi=10.1.1.493.4170&rep=rep1&type=pdf>.
- Hibbitt, K.; Sorensen, Inc. (2000). ABAQUS theory manual. Pawtucket, USA: Hibbitt, Karlsson & Sorensen, Inc.
- Hong, K.N., et al. (2011). Flexural response of reinforced concrete members strengthened with near-surface-mounted CFRP strips. *International Journal of the Physical Sciences*. 6(5): p. 4. DOI: <https://pdfs.semanticscholar.org/1aa7/ab58844b9207956855108c3583dec0514b80.pdf>.
- JCI. (1998). Technical report on retrofit technology for concrete structures., in *Technical committee on retrofitting technology for concrete structures*. p. 24-116.
- JCI. (2003). Technical report on retrofit technology for concrete structures, in *Technical committee on retrofitting technology for concrete structures*. p. 79-97.



ENGLISH VERSION.....

- Khalifa, A.M. (2016).** Flexural performance of RC beams strengthened with near surface mounted CFRP strips. Alexandria Engineering Journal. 55(2): p. 1497-1505.DOI: <https://doi.org/10.1016/j.aej.2016.01.033>.
- Lee-Orantes, F., et al. (2011).** Reinforcement and cathodic protection on corroding concrete elements using carbon fibers based composites. Revista Ingeniería de Construcción. 21(3): p. 169-178.
- Lu, X., et al., (2005).** Bond-slip models for FRP sheets/plates bonded to concrete. Engineering structures, 2005. 27(6): p. 920-937.DOI: <https://doi.org/10.1016/j.engstruct.2005.01.014>.
- Obaidat, Y.T., (2011).** Structural retrofitting of reinforced concrete beams using carbon fibre reinforced polymer. Licentiate Dissertation. Department of Construction Sciences, Structural Mechanics. Lund University, Lund Sweden. 78p.
- Obaidat, Y.T.; Heyden, S.; Dahlblom, O. (2010).** The effect of CFRP and CFRP/concrete interface models when modelling retrofitted RC beams with FEM. Composite Structures. 92(6): p. 1391-1398.DOI.
- Zaki, M.A.; Rasheed, H.A. (2020).** Behavior of reinforced concrete beams strengthened using CFRP sheets with innovative anchorage devices. Engineering Structures. 215: p. 110689.DOI.
- Zhand, D.; Wang, Q.; Dong, J. (2016).** Simulation study on CFRP strengthened reinforced concrete beam under four-point bending. Computers and Concrete 17(3):407-421.DOI: 10.12989/cac.2016.17.3.407.

